CHEMMEDCHEM

CHEMISTRY ENABLING DRUG DISCOVERY

Accepted Article

Title: Sulfurated and oxygenated imidazoline derivatives: synthesis, antioxidant activity and light-mediated antibacterial activity

Authors: Martín Sebastián Faillace, Ana Paula Silva, Antonio Linkoln Alves Borges Leal, Luciana Muratori da Costa, Humberto Medeiros Barreto, and Walter José Peláez

To be cited as: *ChemMedChem* 10.1002/cmdc.202000048

Link to VoR: http://dx.doi.org/10.1002/cmdc.202000048

A Journal of

ChemPubSoc Europe

WILEY-VCH

www.chemmedchem.org

WILEY-VCH

FULL PAPER

Sulfurated and oxygenated imidazoline derivatives: synthesis, antioxidant activity and light-mediated antibacterial activity

Martín S. Faillace, [a] Ana P. Silva, [b] Antonio L. Alves Borges Leal, [c] Luciana Muratori da Costa, [c] Humberto M. Barreto, [c] and Walter J. Peláez*[a]

Dedicated to the memory of Prof. Rivelilson Mendes de Freitas

Abstract: Imidazoline derivatives with different exocyclic substituents were simply prepared from common starting materials. The procedures were carried out under an eco-friendly perspective. The antioxidant activity of these derivatives was explored by different experimental assays, such as ABTS$^{\bullet+}$ and DPPH$^{\bullet}$ scavenging assay, as well as Reducing Power assay. The structural differences are discussed in terms of the results. Then, sulfur analogs showed higher antioxidant activity than the oxygenated counterparts. The same tendency was observed in the microbiological studies, where the same imidazoline compounds were assayed for light-mediated activity against strains of *Staphylococcus aureus* (*S. aureus*) and *Escherichia coli* (*E. coli*). A light-enhanced activity was observed for almost all the sulfurated imidazolines after exposure to UV-A (400-320 nm) light.

Introduction

Imidazolines are a well-known kind of nitrogen heterocyclic compound of therapeutic interest. These structures have shown antimycobacterial,[1] anticonvulsant,[2,3] anticancer,[4,5] and antidiabetic activities.[6] Furthermore, imidazolines are very attractive from a synthetic point of view due to its versatile structures that allow derivatization of new products.

The importance of oxidation in the body and in foodstuffs has been widely recognized. Indeed, an oxidative metabolism is essential for the survival of cells. A side effect of this dependence is the production of free radicals and other reactive oxygen species (ROS) which produce oxidative changes that attack biological macromolecules. When an excess of free radicals is formed, it can overwhelm protective enzymes and cause irreversible damage to DNA and to biological membranes, which leads to destructive and lethal cellular effects. In plants and animals, these free radicals are deactivated by antioxidants. These antioxidants act as inhibitors of the process of oxidation and have diverse physiological roles in the body whose uses go from food preservation to pharmaceutical excipients.[7,8]

Most antioxidant assays follow the same common steps: an initiator induces the oxidation process in the presence of a substrate, which can be measured by chemical, instrumental, or sensory methods. Antioxidant activity cannot be measured directly; consequently, different assays have to be carried out to assess antioxidant activity. Depending on the reactions involved, in vitro assays can roughly be classified as either hydrogen atom transfer (HAT) or single electron transfer (SET) assays. HAT-based assays measure the capability of an antioxidant to quench free radicals by H-atom donation. On the other hand, SET-based assays measure the antioxidant's capacity to reduce an oxidant.[9] To calculate the antioxidant potential, a standard must be used, and the most common standard employed as positive control is Trolox (6-hydroxy-2,5,7,8-tetramethylchroman-2-carboxylic acid), a Vitamin E analog.

In this work, as part of our ongoing project about the biological activities of different compounds,[10–12] in vitro antioxidant properties of different imidazoline derivatives have been evaluated by the inhibition of 2,2-diphenyl-1-picrylhydrazyl (DPPH$^{\bullet}$) as well as 2,2'-azino-bis(3-ethylbenzothiazoline-6-sulfonic acid radical cation (ABTS$^{\bullet+}$) and the Reducing Power assay.

The alarming increase of infections caused by antibiotic-resistant bacteria is the core reason for the search of new antibacterial agents.[13] The photoactivity of several compounds after visible or UV light excitation has been investigated with the aim of finding new prophylactic or therapeutic agents that could be applied in photodynamic protocols for the prevention or treatment of microbial infections.[14,15]

Generally, the antimicrobial photoactivity is a consequence of the generation of reactive oxygen species through direct production of singlet oxygen or can result from the photoreaction with DNA, as is the case with intercalating agents such as furocoumarins.[16]

Herein, we present the synthesis of eleven compounds which belong to a family of 1,3-diaza heterocycles. Due to their potential pharmacological applications, the influence of structural modifications was analyzed by exploring specific biological activities. The antioxidant activity through different in vitro assays has been studied. Moreover, the light-mediated antimicrobial activity has been investigated to evaluate its potential to create photoactive

[a] Dr. M. S. Faillace, Dr. W. J. Peláez,
Departamento de Físicoquímica, Facultad de Ciencias Químicas.
Universidad Nacional de Córdoba. CONICET-INFIQC
Haya de la Torre s/n. Pabellón Argentina, Ciudad Universitaria.
Córdoba, Argentina. X5000HUA
e-mail: walter.pelaez@unc.edu.ar
[b] Dr. A. P. S. C. L Silva,
Federal University of Piaui, Pharmacy Course.
Campus University Professor Petrônio Portella, Ininga
Neighborhood. Teresina, Piaui, Brazil. 64049-901
[c] Ms. A. L. Alves Borges Leal, Dr. L. Muratori da Costa, Dr. H. M. Barreto,
Federal University of Piaui. Laboratory of Research in Microbiology.
Campus University Professor Petrônio Portella, Ininga
Neighborhood. Teresina, Piaui, Brazil. 64049-901

Supporting information for this article is given via a link at the end of the document.

compounds for use in photodynamic therapy of bacterial infections.

Results and Discussion

Imidazoline derivatives are known since the 20th century due to their biological activities. Despite the fact that the hydantoin ring does not have any relevant activity, some examples with substituents at the C5 position have different applications in the pharmaceutical[17] and agrochemical industries.[18] However, less attention has been given to the exploration of the thio-analogs. The synthesis of the compounds have already been reported,[3,19,20] but the conventional synthesis could still be improved by microwave irradiation (MW) in order to perform eco-friendly synthetic procedures. These molecules have been chosen for the antioxidant studies due to the number of H atoms available as well as the location of substituents, which allows the stabilization of the radical formed after the antioxidant activity.[21] To the best of our knowledge, neither the antioxidant nor the microbiological photoactivity of these synthesized compounds has been explored before.

Chemistry

Ten derivatives with different exocyclic substituents were synthesized by Knoevenagel condensation[20] and were split between oxygenated (**5a**-**c**, **g**, **i**) and sulfurated (**5d-f**, **h**, **j**) compounds. Beside these, another 1,3-heterocycle analog preparation was made with a new phenyl group on N-3 (**5k**), Scheme 1. The purification was executed without difficulties using column chromatography and the purity was assessed by HPLC. The identification and characterization were done by the usual spectroscopic techniques (NMR, GC-MS), Supporting information, section 3.

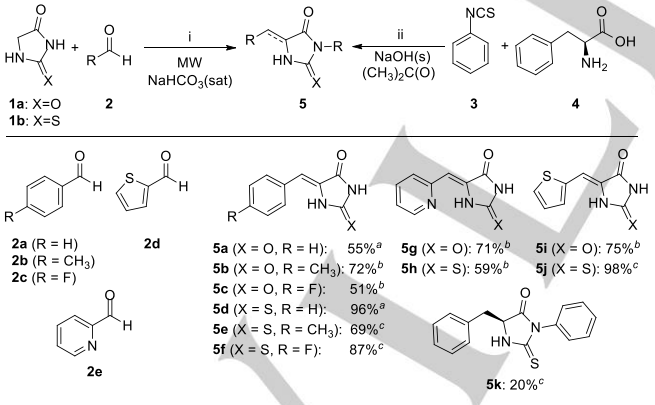

Scheme 1. Synthesis of imidazoline derivatives. The reaction conditions are indicated in the Experimental section. Yields were determined based on: [a]UV-Vis calibration curve, [b]GC-MS, [c]Mass yield after purification.

As mentioned before, with the aim of designing green synthetic procedures, the synthesis of (*Z*)-5-benzylidene-imidazolidine-2,4-dione **5a** was carried in a microwave oven, which changes in the reaction media from the conventional methodologies in the literature.[3] It was observed that the microwave reaction of compound **5a** could be done in a one-step synthesis. For instance, in Figure 1, it can be observed that the yields increased when some of the co-solvents were removed. Furthermore, the environmental factor (E-factor) was calculated for each synthesis as the ratio of the mass of waste per mass of product. This means that when the amount of waste generated during the synthetic procedure decreases, the E-factor becomes smaller.[22] The results for this green parameter show that it decreases drastically when the solvents are removed, with an increment in the yield, Figure 1.

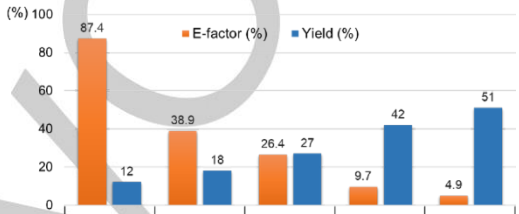

Methodology:	i	ii	iii	iv	v
Water (mL)	2.0	2.0	-	-	-
Diethanolamine (mL)	0.15	0.15	0.15	-	-
Ethanol (mL)	1.0	2.0	2.0	2.0	-
$NaHCO_3$ (sat) (mL)	1.0	1.0	1.0	1.0	1.0
Hydantoin **1a** (mmol)	2.1	4.2	4.0	4.3	4.1
Benzaldehyde **2a** (mmol)	2.7	4.2	4.2	4.5	4.5
MW time (min)	5	10	20	10	10
MW temperature (°C)	120	120	120	140	140

Figure 1. Optimization of synthetic reaction media for **5a**.

Therefore, with the optimum reaction media, the best microwave conditions were explored in order to increase the yields. Accordingly, the yields were determined at different temperatures and irradiation times. As a result, in Figure 2, it is plotted yields vs microwave conditions for compound **5d** where the maximum yield for this synthesis was 98 % at 130 °C and 12.5 min. The optimization for another compound (**5a**) is shown in the Supporting information, page 3.

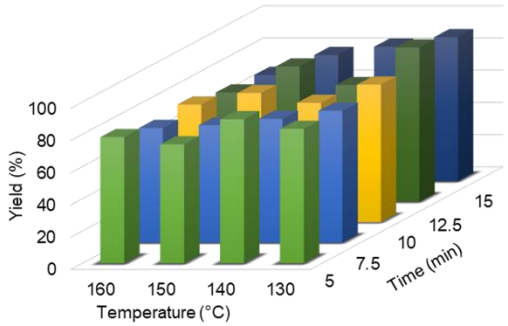

Figure 2. Microwave synthesis optimization for compound **5d**. The procedure was carried out from **1b** (2.0 mmol) and **2a** (3.9 mmol) in 1 mL of $NaHCO_3$ (sat).

As it was already reported for compound **5d**,[23] *Z* and *E* isomers can be obtained for the benzylidene thioimidazolines. The preferred product has *Z* geometry, and the *Z*/*E* ratio can be

modified by irradiation with light until the photostationary state is reached, at which point this ratio does not vary with the continuous irradiation. By ^{1}H-NMR, we calculated the contribution of each isomer for the sulfur compounds **5d**-**f**, **5h**, and **5j**. Therefore, the population of each isomer in the thermal equilibrium and in the photostationary state is detailed in Table 1.

Table 1. Population of each isomer in the thermal equilibrium and in the photostationary state

Compound	Thermal equilibrium		Photostationary state	
	Z (%)	*E* (%)	*Z* (%)	*E* (%)
5d	98	2	58	42
5e	100	0	52	48
5f	96	4	59	41
5h	97	3	36	64
5j	97	3	67	33

The contribution of each isomer was determined by ^{1}H-NMR from solutions of each compound in DMSO-d_6. The solutions were irradiated with a lamp at 366 nm until achieving the photostationary state.

As mentioned before, the *Z* conformation is highly preferred. However, after irradiation, the population of *E* isomer increases as shown in Table 1. In particular, for compound **5h** with a thiophene substituent, the population becomes inverted: the concentration of *E* isomer is then higher than the *Z* conformation.

Antioxidant assays

DPPH• is one of the few stable and commercially available organic nitrogen radicals with a deep purple color. This radical leads to loss of color at 517 nm when it reacts with a reducing agent.[24]

The radical scavenging power of the synthesized compounds (**5a**-**k**) was analyzed through the reaction with DPPH•. The assay was carried out in triplicate at three concentration levels. The DPPH• inhibition percent was calculated from the difference of absorbance of the negative control and the sample. The results are expressed in Table 2.

As expected, the antioxidant activity increases with the sample concentration. Compound **5k** showed the maximum DPPH• inhibition among the tested samples. It can be attributed to the highest conjugation of this compound due to the phenyl substituent group on N-3 in the heterocycle moiety. Moreover, it is remarkable that the rest of the thio-derivatives (**5d**-**f**, **h**, **j**) presented a higher antioxidant activity than the oxo-analogs (**5a**-**c**, **g**, **i**).

In order to shed light on these tendencies, two complementary assays were employed to clarify the mechanism operating in the antioxidant ability of the studied compounds: ABTS•$^+$ scavenging and Reducing Power.

ABTS is a colorless compound. Its radical cation, ABTS•$^+$, can be obtained directly by the oxidation of ABTS with potassium persulfate ($K_2S_2O_8$).[25] The absorption of this blue/green chromophore peaks at 734 nm, which is the wavelength used for the quantification. Thus, the extent of decolorization as a percentage inhibition of the ABTS•$^+$ is calculated in relation to the negative control, similarly to the DPPH• inhibition percent. It is well known that ABTS•$^+$ tests go through a SET process while DPPH• assays were believed to only involve a HAT mechanism. However, we have demonstrated that DPPH• can be quenched by both electron and atom transfers.[10]

Table 2. DPPH• scavenging power of compounds **5a**-**k** and Trolox

Compound	X	100 µM		250 µM	
		Mean	SEM	Mean	SEM
5a	O	0.1	0.8	0.4	0.2
5b	O	0.3	0.1	1.1	0.3
5c	O	1.3	0.6	3.7	0.5
5d	S	7	1	15.7	0.1
5e	S	12.65	0.09	26	2
5f	S	13.6	0.1	23.6	0.2
5g	O	1.7	0.3	1.5	0.4
5h	S	30.4	0.7	35.24	0.09
5i	O	0.5	0.3	0.2	0.1
5j	S	44	3	50.1	0.6
5k	S	37	2	54	2
Trolox		52	5	64	3

Experiment involving triplicate data points. SEM: Standard Error of the Mean.

On the other hand, the Reducing Power assay relies on some specific chemical reactions. If a compound has antioxidant potential, it would react with potassium ferricyanide ($K_3[Fe(CN)_6]$), reducing it to $K_4[Fe(CN)_6]$, which, as a consequence, reacts with ferric chloride ($FeCl_3$) to form an intensely colored Prussian blue complex ($Fe_7(CN)_{18}$). This complex has an intense absorption band at 700 nm. Though, the increment of this band after the addition of ferric chloride indicates a higher antioxidant power of the tested sample. From the absorbance measurements, it was possible to calculate the Increase in Reducing Power (IRP).[7]

The antioxidant results of these assays for compounds **5a**-**j** are shown in Figures 3-5 at the same concentration level of 500 µM. The same tendency about the efficiency of sulfur compounds (**5d**-**f**, **h**, **j**) is observed in all assays.

Additionally, in Figure 6, we compare the antioxidant activity of compound **5k**, which is a benzyl and N-phenyl derivative, at three concentration levels. In all the tests the scavenging power is similar to the positive control (Trolox), which demarks this compound as the best antioxidant from the synthesized heterocycles.

Therefore, the sulfur atom must be involved in the scavenging of the free radical, probably due to its physicochemical properties like atomic size, electronegativity, and polarizability. Furthermore, the sulfur compounds are known to be in equilibrium with their thiol tautomer. In fact, thiols serve as cellular redox buffers, reducing ROS and, in doing so, maintaining the overall redox state of the cell.[26] In this sense, a deep analysis was encouraged to explain the experimental results.

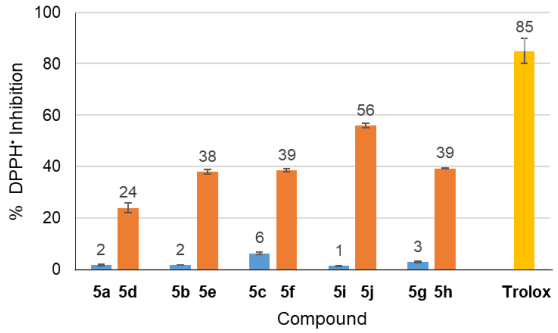

Figure 3. DPPH• inhibition of sulfurated compounds and their oxygen-isosteres at 500 µM.

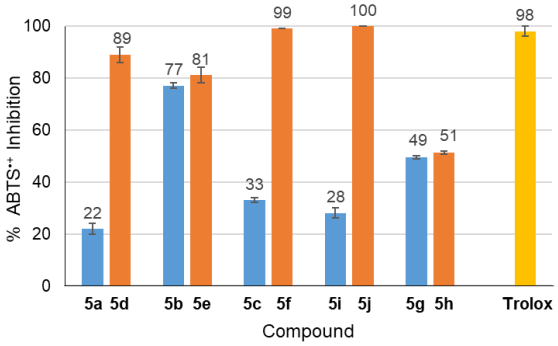

Figure 4. ABTS•+ inhibition of sulfurated compounds and their oxygen-isosteres at 500 µM.

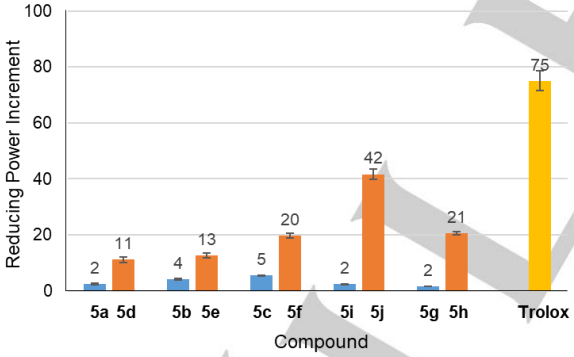

Figure 5. Reducing Power Increment of sulfurated compounds and their oxygen-isosteres at 500 µM.

Firstly, the frontier molecular orbitals of sulfurated compounds were studied due to their important role in the processes where radicals react with uncharged molecules.

Figure 7 shows the HOMO (Highest Occupied Molecular Orbital) and LUMO (Lowest Unoccupied Molecular Orbital) of sulfurated and oxygenated compounds as well as the SOMO (Singly Occupied Molecular Orbital) of DPPH•. It is remarkable that DPPH•, an electrophilic radical, could strongly interact with the HOMO of the uncharged imidazoline derivatives. In addition, the HOMO of sulfurated compounds is closer in energy values to the SOMO of DPPH• than the oxygenated counterparts, as highlighted in Figure 7.

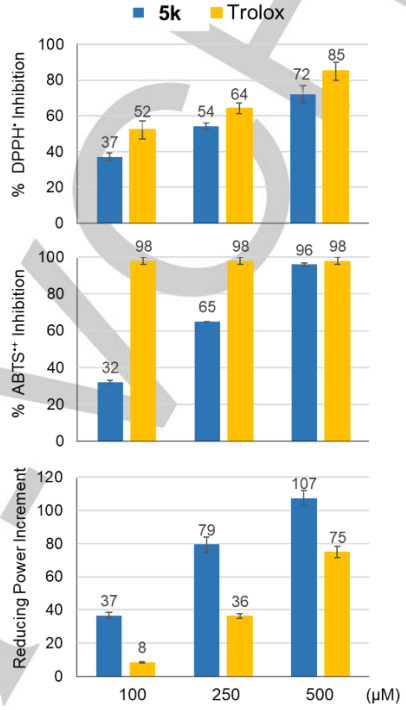

Figure 6. Antioxidant assays with compound **5k** at different concentrations.

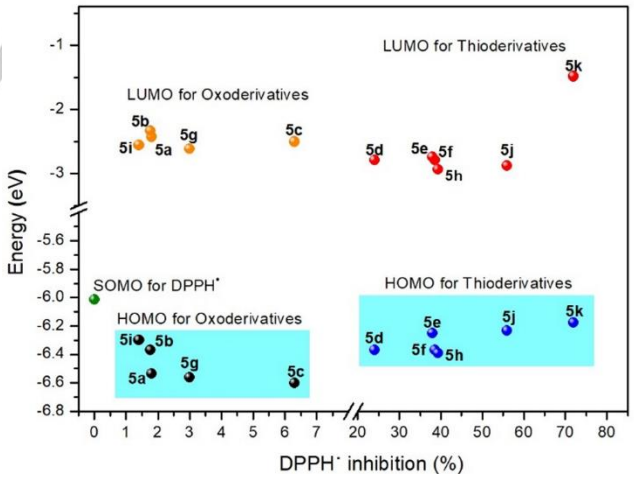

Figure 7 DPPH• inhibition vs HOMO and LUMO of the oxo- and thio- derivatives.

As described above, there are different possible mechanisms through which antioxidants can deactivate free radicals. One of them is the hydrogen atom transfer (HAT), whose feasibility could be estimated by calculating the reaction enthalpy

of radical formation in the abstraction of a hydrogen atom (Equation 1). On the other hand, the single electron transfer (SET) is also a possible mechanism, in which case a radical cation is formed followed by a proton transfer (PT) (Equation 2).

$$A\text{-}H + FR^{\bullet} \rightarrow A^{\bullet} + FR\text{-}H \qquad \text{Eq. 1}$$

$$A\text{-}H + FR^{\bullet} \rightarrow (A\text{-}H)^{\bullet+} + FR^{-} \rightarrow A^{\bullet} + FR\text{-}H \qquad \text{Eq. 2}$$

These processes can be estimated by employing the bond dissociation energy (BDE), which represents the reaction enthalpy of the HAT in the first case, and the ionization potential (IP) that represents the enthalpy of the SET in the second case. A low IP implies an easy extraction of the electrons from the system while a low bond dissociation energy (BDE) raises the possibility of a HAT mechanism for its antioxidant activity.

Due to the nature of the component, DPPH$^{\bullet}$ can react by abstracting an H atom or an electron through a HAT or SET mechanism, respectively. BDE and IP were calculated for **5d** and **5k** as an example of benzylidene- and benzyl- counterparts to elucidate the mechanism operating in their scavenging processes. According to the B3LYP/6-311+G(d,p) calculations for the different possibilities of H abstraction, the lowest BDE for compound **5d** was obtained by the abstraction of H from the thiol tautomer (Table 3, entry 4). For compound **5k**, it was obtained from the H abstraction from the C-5 (Table 3, entry 8). These values are similar to well-known antioxidants that react via HAT (Table 3, entries 5, 6, 11, 12).

Table 3. BDE calculated by Gaussian09 for the possible radicals of compounds **5d** (entries 1-4) and **5k** (entries 7-10).

Entry	A$^{\bullet}$	DBE[a] (kJmol^{-1})	*Entry*	A$^{\bullet}$	DBE[a] (kJmol^{-1})
1	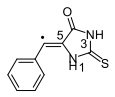	466	*7*	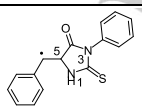	363
2	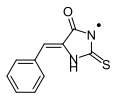	470	*8*	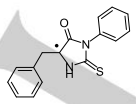	311
3	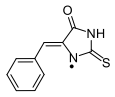	388	*9*	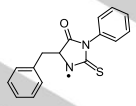	361
4	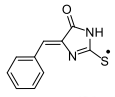	292	*10*	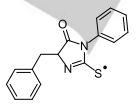	339
5	Curcumin$^{\bullet}$	357[27]	*11*	α-tocopherol$^{\bullet}$	327[28]
6	Epigallocatechin gallate$^{\bullet}$	297[29]	*12*	Caffeic acid$^{\bullet}$	321[30]

[a] B3LYP/6-311+G(d,p).

On the other hand, IP was calculated for all sulfurated compounds and is substantially higher than the corresponding BDE values (Table 4), allowing us to propose HAT as a probable mechanism of action for scavenging DPPH$^{\bullet}$, Schemes 2 and 3.

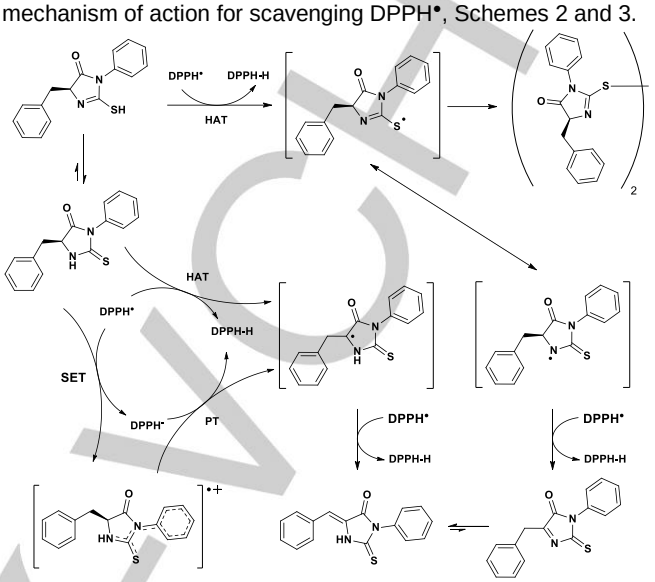

Scheme 2. Proposed mechanism of antioxidant action of compounds **5k**.

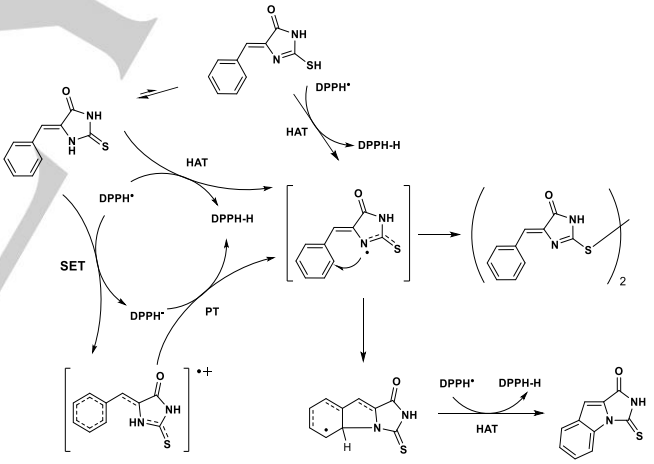

Scheme 3. Proposed mechanism of antioxidant action of compounds **5d**.

Attempts to determine the molar efficiency of the antioxidants against DPPH$^{\bullet}$ were made, but given that the kinetics of the reactions are very slow, the stoichiometry is difficult to interpret.[31]

These results let us envisage that all compounds might undergo oxidation via a stepwise mechanism when they are acting as scavengers of ABTS$^{\bullet+}$ and in the Reducing Power assay. The highest IP and positive ΔIP calculated is found for the EWG (Electron Withdrawing Group) substituent in the benzylidene-moiety (Table 4, entry 1). It is due to the fact that the EWG destabilizes radicals and radical cations, resulting in the increase of IP. Nevertheless, negative ΔIP values and lower IP are found

for EDG (Electron Donating Group) (Table 4, entry 3), heterocycles substituents (Table 4, entry 4 and 6), and for the benzylic counterpart which possesses an extra phenyl- in the heterocyclic moiety (Table 4, entry 5). In these cases, the decrease in IP and negative ΔIP are the combined result of the cation radical stabilization and the parent molecule destabilization.

Besides the fact that both kinds of systems (benzyl- and benzylidene-) would react through SET, the spin density distribution of both radical cations formed from compounds **5d** and **5k** should be different. The optimized bond distances, as well as the electron spin density distribution, are presented in Table 5 and Figure 8. Both radical cations show a shortening of the C2-N3 bond (Table 5, entry 3). Nonetheless, all remaining bonds show the opposite trend.

Table 4. IP for the possible radical cations of all sulfurated compounds.

Entry	A-H$^{\bullet+}$	IP[a, b]	ΔIP[c]	*Entry*	A-H$^{\bullet+}$	IP[a, b]	ΔIP[c]
1	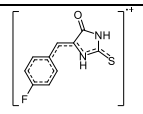	800	7	*4*	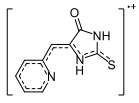	759	-34
2	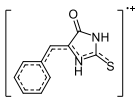	793	0	*5*	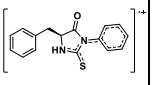	751	-42
3	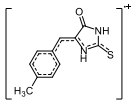	775	-18	*6*	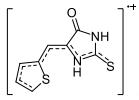	739	-54

[a] calculated by Gaussian09 B3LYP/6-311+G(d,p), [b] kJmol^{-1},
[c] ΔIP = IP **5d,e,f,h,j,k** - IP **5d**

Table 5. Bond distances of sulfureted benzyl- and benzylidene- derivatives.

Entry	Bond[a]	**5d**[b]	**5d**$^{\bullet+}$[b]	**5k**[b]	**5k**$^{\bullet+}$[b]
1	N1-C2	1.362	1.400 ↑	1.355	1.326 ↓
2	C2-S	1.665	1.640 ↓	1.653	1.704 ↑
3	C2-N3	1.378	1.369 ↓	1.408	1.369 ↓
4	C5-N1	1.399	1.352 ↓	1.451	1.469 ↑
5	C5-C6	1.349	1.387 ↑	1.543	1.546 ≈
6	N3-R1´	1.010	1.012 ≈	1.435	1.424 ↓

[a] calculated by Gaussian09 B3LYP/6-311+G(d,p), [b] Å.

This can be explained by the different kind of stabilization and nature of the radical cation formed. After the subtraction of an electron (first step, Equation 2), the spin density of **5d**$^{\bullet+}$ is similarly distributed among the ylidene-moiety. In contrast, for compound **5k**, a benzyl derivative, the spin density is distributed from the heterocycle towards the N-phenyl moiety.

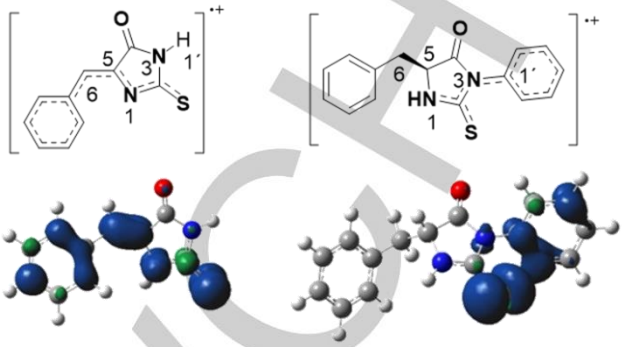

Figure 8. The spin density of **5d**$^{+\bullet}$ and **5k**$^{+\bullet}$. The structures were generated with Gausview 5.0, from Gaussian09 at B3LYP/6-311G+(d,p).

Light-mediated antimicrobial activity

The light-mediated antibacterial activities of the different heterocycles were evaluated using the agar diffusion method irradiating the system with UV-A light (400-320 nm). Through this practical method, the photoactivity of all compounds **5**(**a**-**k**) can be verified by observing the inhibition zones.

From the results presented in Table 6, it can be concluded that all derivatives were inactive in the absence of light against *S. aureus* and *E. coli* strains. These important results indicate that the activation of a bacteriostatic or bactericidal effect is only achieved by the absorption of light at a specific wavelength.

Moreover, it can be seen that, after irradiation, the oxygenated derivatives did not show photoactivity against the tested strains. This can be attributed to the physicochemical characteristics of the former compounds, which have their absorption maxima at a shorter wavelength (350-200 nm) and do not absorb the irradiating light.

In contrast, almost all sulfurated derivatives (**5d**, **5f**, **5h** and **5j**) show inhibition of the growth of *S. aureus* after irradiation and none of the tested molecules showed activity of *E. coli.* Here again, the physicochemical properties of sulfurated counterparts, which are presented in Table 7, clearly explain the obtained results. The relevant parameters are the experimental UVmax of absorption of each compound, the Log (1/S) (where S is the compound solubility in aqueous media), the lipophilicity parameters (LogP and LogD, that take into account the capacity of the substances to interact with cell membranes) and the distribution of species (calculated at pH=7.4). Lipophilicity studies are relevant to know if a molecule can interact with cell membranes. The Log P value of Metoprolol (LogP=1.72), which is 95% absorbed in the intestinal tract and possesses a high cell membrane permeability, has been used as a reference to estimate the permeability of a vast number of drugs.[32] Taking this compound as a reference, the LogP and LogD of all benzylidene derivatives studied were calculated (Table 7).

The experimental UV data helps to understand why compound **5k** is not active when irradiated. The most important reason is that **5k** is a benzyl- derivative and does not have an

exocyclic double bond in the heterocyclic moiety, which makes its UVmax of absorption out of the range of UV-A irradiation. The inactivity of compound **5e** could be attributed to the fact that, similarly to **5k**, it has low water solubility compared to the other derivatives, which can preclude the diffusion in the agar media.

Table 6. The diameter of inhibition zones (mm) of the imidazoline derivatives after UV-A irradiation.

Compound	*S. aureus* ATCC 25923	*E. coli* ATCC 25922
5a	6.2	6.2
5b	6.2	6.2
5c	6.2	6.2
5d	10.1[d]	6.2
5e	6.2	6.2
5f	9.6[d]	6.2
5g	6.2	6.2
5h	8.2[d]	6.2
5i	6.2	6.2
5j	7.3[d]	6.2
5k	6.2	6.2
Ampicillin[a]	41.3	19.8
8-MOP[b]	12.9	8.2
DMSO[c]	6.2	6.2

The diameter for the dark inhibition zone was 6.2 mm (disk diameter) for all the tested compounds, except for Ampicillin which was 41.3 and 20.7 mm for *S. aureus* and *E. coli*, respectively. [a] Ampicillin (10 µg/disk): positive standard; [b] 8-MOP: 8-methoxypsoralen (5 µg/disk) light-mediated antimicrobial activity positive control; [c] DMSO (10 µL/disk): solvent control. [d] Significant statistical difference considering $p \leq 0.05$ to the t test using independent samples.

Table 7. Chemical properties of sulfur imidazolines

Compound	UVmax absorption (nm) [a]	Log(1/S)[b]	LogP[c]	LogD[c]	α[d]
5d	356, 368	2.98	2.26±0.75	2.06±0.75	62 + 38
5e	358, 375	3.29	2.72±0.75	2.54±0.75	65 + 35
5f	352, 367	2.86	2.27±0.75	2.04±0.75	58 + 42
5h	363, 381	1.49	0.9±0.75	0.16±0.75	17 + 83
5j	372,390	2.99	2.08±0.75	1.76±0.75	48 + 52
5k	269	4.01	3.08±0.75	3.08±0.75	100 + 0

[a] in ACN. [b] Calculated in water at pH=7.4. [c] LogP and LogD are the distribution of species calculated between organic and aqueous phase at pH=7.4. Log P considers only the neutral species while LogD includes the neutral as well as the mono-charged species. [d] The percent of neutral plus mono-charged species.

In addition, all active compounds presented LogP and LogD values between 1.76 and 3.08, which would allow them to intercalate into the plasma membrane and increase its permeability. Interestingly, our results showed that intrinsic antibacterial activity does not increase with higher lipophilicity (Table 6 and Table 7). From this analysis, we can suggest that the antibacterial activity of the tested benzylidene derivatives could be related to another kind of mechanism that involves cell damage.

It is important to highlight that an antioxidant can protect biomolecules against oxidative damage while promoting at the same time the oxidation of other targets such as DNA, lipids, and proteins.[33] The pro-oxidant effects of antioxidants are especially dependent on the composition of the medium in which the antioxidant measurement is made. Pro-oxidant states may vary based on their concentrations, the inducing agent, and the target cell.[34] This is presumably due to the variations in quantity, type, and intra- and extracellular distribution of the reactive oxygen species. The different classes of agents and mechanisms that can cause pro-oxidant states have been well documented.[35]

In this case, the inducing agent that produces a pro-oxidant effect is the UV-A irradiation. We described the interaction of **5d** with light at the same wavelength in detail.[23] Our findings suggest that benzylidene derivatives have a *Z*→*E* photoisomerization process when irradiated at 366 nm. However, the opposite reaction (*E*→*Z*) is a thermal reversion process that can occur via a triplet state reached through an intersystem crossing between S_0 and T_1 surfaces (only thermal energy near room temperature is responsible for that reversion).[23] For this reason, we postulate herein that pro-oxidation processes are generated due to the *Z*→*E* isomerization reactions which are capable of converting triplet oxygen ($^3O_2$) into singlet oxygen ($^1O_2$), one of the most reactive species of oxygen. Thus, the singlet oxygen can react with biomolecules to yield hydroperoxides through the following sequence of events (Equations 3-7):[23]

$$S_{0,Z} + h\nu \rightarrow S_{2,Z} \rightarrow {}^1S_{1,Z} \quad \text{Eq. 3}$$

Vertical excitation of $S_{2,Z}$ followed by CI with $S_{1,Z}$ (Conical Intersection).

$$S_{1,Z} \rightarrow S_{0,E} \quad \text{Eq. 4}$$

Photochemical isomerization *Z*→*E* by CI (Conical Intersection).

$$S_{0,E} \rightarrow T_{1,Z} \quad \text{Eq. 5}$$

Thermal reversion *E*→*Z* by ISC (InterSystem Crossing).

$$T_{1,Z} + {}^3O_2 \rightarrow {}^1O_2 + S_{0,Z} \quad \text{Eq. 6}$$

Transfer of energy excess from $T_{1,Z}$ to $^3O_2$.

$$^1O_2 + RH \rightarrow ROOH \quad \text{Eq. 7}$$

Hydroperoxide formation by $^1O_2$.

Where $S_{1,Z}$ is the first singlet-state of *Z* benzylidene isomer, $S_{2,Z}$ the second singlet-state of Z benzylidene isomer, $S_{0,E}$ and $S_{0,Z}$ the ground-state of *Z* and *E* benzylidene isomers, and $T_{3,Z}$ the triplet-state of *Z* benzylidene isomer.

In order to determine the formation of $^1O_2$ in our microbiological assays, we performed an independent experiment. In presence of ROS, L-Cys yields the insoluble cystine (Cys-Cys) by the formation of a disulfide bridge, Equation 8.[36] We assayed this experiment using **5d** as a sensitizer to generate ROS. After

the irradiation of an oxygenated solution of **5d** in presence of L-Cys, a precipitate was formed. We concluded that the Cys-Cys formation in this experiment comes from the presence of $^1O_2$ in the solution.

2 L-Cys + [O] → Cys-Cys Eq. 8

In this sense, we postulate that ROS are generated from **5d**, **5f**, **5h**, and **5j** after irradiation with UV-A in the photo-induced assays. Nevertheless, it was important for us to understand why only the *S. aureus*, a Gram-positive strain, was affected for the generation of ROS while Gram-negative bacteria such as *E. coli* was not. Maybe the clue lies precisely in the kind of cell wall that these microorganisms possess.

As it is well known, the Gram-positive cell wall is constituted by a thick peptidoglycan layer that contains polyalcohols, some of which are responsible for binding the peptidoglycans to the cytoplasmic membrane. In spite of the rigidity caused by peptidoglycans to the bacterial cell wall, it is still relatively porous and does not constitute a barrier for small substrates. In addition, peptidoglycans work as an osmotic stabilizer and prevent lysis of the bacteria due to differences in the ion concentrations in the cytosol. On the contrary, the Gram-negative cell wall contains an additional outer membrane which gives an extra permeability barrier composed of phospholipids and lipopolysaccharides that protect the system from the external environment. However, for both types of strains, neither the outer membrane nor the peptidoglycan wall provide resistance to antimicrobial agents. The resistance mechanism can rely, for instance, on the overexpression of efflux pumps.[37]

Taking this into account, we propose that benzylidene derivatives diffuse through the pores of the peptidoglycan wall where they exert their pro-oxidant activity. Then, the oxidative property of singlet oxygen disrupts the methylene substituents of the peptidoglycan wall under our experimental conditions.[38]

According to the arguments above, the photoactivity of thiohydantoins **5d**, **5f**, **5h,** and **5j** is related to the generation of ROS after the absorption of UV-A light, causing damage in the peptidoglycan layer of *S. aureus*, Figure 9.

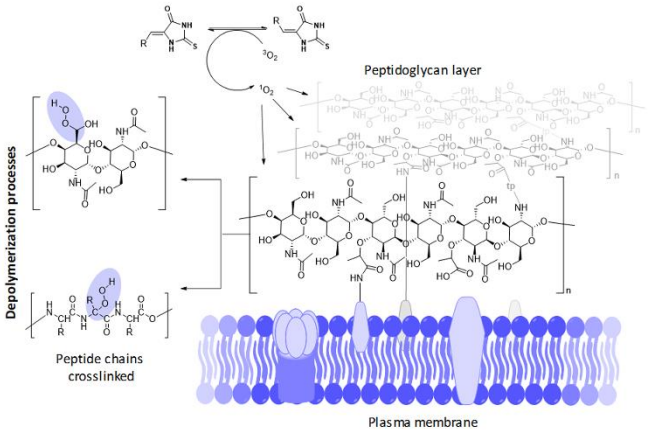

Figure 9. Proposed photo-activity mechanism of the benzylidene derivatives against *S. aureus*.

Conclusions

In the present study, we have synthesized different imidazoline compounds from an eco-friendly perspective. These molecules can be of pharmaceutical interest due to their interesting activities screened in this work.

The antioxidant assays demonstrated that sulfur imidazolines have higher antioxidant activity than their oxygenated analogs. Therefore, the incorporation of a sulfur atom in these heterocycles increases the radical scavenging activity. Further studies on a molecular level must be done for a better understanding of the whole picture of this system. For instance, the redox potential of each compound should be measured as previously demonstrated for some oxazine compounds, where the antioxidant activity takes place through electron transfer processes.[10] Moreover, the saturated benzyl derivative **5k** that possesses a phenyl substituent at the heterocycle moiety resulted in an increase of antioxidant activity, which can be attributed to the higher system conjugation and the feasibility to go through a HAT mechanism as a radical scavenger.

It is worth to note the variations between the different antioxidant assays. Indeed, they highlight the importance of performing independent experiments which can lead to general conclusions in this kind of study.

Moreover, some of the thioimidazoline derivatives resulted to be active against *S. aureus* after irradiation with UV-A light. For this reason, these photo-active compounds could be considered in photodynamic therapy as well as to eliminate pathogens from material and surfaces as a light-mediated disinfectant.

Experimental Section

Synthesis of imidazoline derivatives

General methods: All compounds were characterized by standard spectroscopic techniques (^{1}H NMR, ^{13}C NMR, ^{19}F NMR, HMBC, HSQC, UV) and mass spectrometry. All data are in agreement with the proposed structures. NMR spectra were recorded with a Bruker Avance II 400 MHz spectrometer (BBI probe, z gradient) (^{1}H at 400.16 MHz, ^{13}C at 100.56 MHz and ^{19}F-NMR at 376.53 MHz). Chemical shifts are reported in parts per million (ppm) downfield from TMS. The spectra were measured at 22 °C. Absorption spectra of the solutions were recorded with a UV-1601 Shimadzu spectrophotometer using a quartz cell with an optical path length of 1 cm and acetonitrile as solvent. Gas chromatography/mass spectrometry (GC-MS) analyses were performed with a Shimadzu GC-MS-QP 5050 spectrometer equipped with a VF column (30 m x 0.25 mm x 5 µm) by using helium as eluent at a flow rate of 1.1 mL min^{-1}. The injector and ion source temperature was 280 °C. The pressure in the MS instrument was 10^{-5} Torr, precluding ion-molecule reactions from taking place, and MS recordings were made in the electron impact mode (EI) at ionization energy of 70 eV.

Microwave synthesis of compounds 5(a-j) were performed in cylindrical quartz tubes located in an Anton Paar Monowave 300 reactor (2.455 GHz), with adjustable power within the range 0-300 W and a waveguide (monomode) fitted with a stirring device and an IR temperature detector. Each microwave synthesis is detailed in Table 8.

Synthesis of compound 5k: L-phenylalanine (4.33 mmol) was dissolved in 60 mL of a mixture of acetone : water (50:50). Then, phenyl-isothiocyanate (4.72 mmol) was added, followed by NaOH (266 mg) dissolved in 3 mL of water. The mixture was heated under reflux conditions during 2 h and, after one week, the desired compound crystallized at room temperature.

Table 8. Microwave synthetic procedure.

Compound	Heterocycle (mmol)	Aldehyde (mmol)	$NaHCO_3$(sat) (mL)	Microwave	
				Temp. (°C)	Time (min)
5a	**1a** (2.03)	**2a** (3.90)	1	150	10
5b	**1a** (4.03)	**2b** (7.60)	1	140	10
5c	**1a** (4.00)	**2c** (8.39)	1	140	30
5d	**1b** (1.75)	**2a** (3.90)	1	130	12.5
5e	**1b** (13.8)	**2b** (28.9)	7.5	140	45
5f	**1b** (12.6)	**2c** (25.2)	7.5	140	90
5g	**1a** (4.03)	**2d** (7.60)	1	140	30
5h	**1b** (13.8)	**2d** (26.1)	7.5	140	90
5i	**1a** (4.39)	**2e** (8.37)	1	160	10
5j	**1b** (13.8)	**2e** (28.3)	7.5	140	80

Compound 5a: ^{1}H-NMR (acetone-d_6) δ (ppm) = 6,52 (s, 1H); 7,34 (t,t; J_1=7,75 Hz; J_2=1,59 Hz; 1H); 7,43 (dd,t; J_1=7,75 Hz; J_2=1,59 Hz; 2H), 7,63 (dd, J_1=7,75 Hz; J_2=0,54 Hz; 2H), 9,45 ($s_{(movil)}$, 1H); 10,05 ($s_{(movil)}$, 1H). ^{13}C-NMR (acetona-d_6) δ (ppm) = 109,97; 129,23; 129,71 (2C); 130,00 (2C); 130,95; 134,37; 155,42; 165,57. GC-MS (100-250 °C, 15 °C/min; R_t: 10,852 min): m/z (%) = 189 (M+1, 17), 188 (M^+, 69), 117 (100), 90 (38), 89 (40), 63 (7), 43 (26).

Compound 5b: ^{1}H-NMR (acetone-d_6) δ (ppm) = 2,35 (s, 3H); 6,49 (s, 1H); 7,25 (d; J_1=8,10 Hz; 2H); 7,52 (d; J_1=8,10 Hz; 2H), 9,35 ($s_{(movil)}$, 1H); 9,98 ($s_{(movil)}$, 1H). ^{13}C-NMR (acetone-d_6) δ (ppm) = 21,27; 109,97 (2C); 129,23; 129,71 (2C); 130,00 (2C); 130,95; 134,37; 155,42; 165,57. GC-MS (100-250 °C, 15 °C/min; R_t: 10,852 min): m/z (%) = 203 (M+1, 11), 202 (M^+, 100), 131 (96), 116 (9), 104 (24), 103 (17), 91 (9), 78 (13), 77 (16), 65 (6), 51 (8).

Compound 5c: ^{1}H-NMR (acetone-d_6) δ (ppm) = 6,51 (s, 1H); 7,20 (t,t; J_1=8,78 Hz; J_2=2,41 Hz, 2H); 7,68 (m; 2H), 9,49 ($s_{(movil)}$, 1H); 10,10 ($s_{(movil)}$, 1H). ^{13}C-NMR (acetone-d_6) δ (ppm) = 108,29; 116,60 (J_2 $^{C\text{-}F}$=22,22 Hz; 2C); 129,10; 130,84; 132,13 (J_3 $^{C\text{-}F}$=8,75 Hz; 2C); 155,53; 163,27 (J_1 $^{C\text{-}F}$=247,73 Hz); 165,57. ^{19}F-NMR (acetone-d_6) δ (ppm): -113,76. GC-MS (200-250 °C, 10 °C/min; R_t: 7,222 min): m/z (%) = 206 (M^+, 99), 136 (9), 135 (100), 134 (15), 108 (54), 107 (37), 81 (5), 57 (8).

Compound 5d: ^{1}H-NMR (acetone-d_6,) δ (ppm) = 6,57 (s, 1H); 7,42 (m, 3H); 7,72 (d; J_1=7,15 Hz; 2H). ^{13}C-NMR (acetone-d_6) δ (ppm) = 112,04; 129,17; 129,78; 130,00; 130,57; 165,80; 179,82. GC-MS (100-250 °C, 15 °C/min; R_t: 8,427 min): m/z (%) = 205 (M+1, 7), 204 (M^+, 68), 188 (19), 172 (10), 118 (16), 117 (100), 116 (20), 91 (7), 90 (44), 89 (40), 63 (13), 43 (8).

Compound 5e: ^{1}H-NMR (DMSO-d_6) δ (ppm) = 2,32 (s, 3H); 6,44 (s, 1H); 7,23 (d; J_1=8,10 Hz; 2H); 7,65 (d; J_1=8,10 Hz; 2H), 12,12 ($s_{(movil)}$, 1H); 12,24 ($s_{(movil)}$, 1H). ^{13}C-NMR (acetone-d_6) δ (ppm) = 21,00; 111,81 (2C); 127,00; 129,41 (2C); 130,19 (2C); 139,24; 165,95; 178,95. GC-MS (100- 250 °C, 15 °C/min; R_t: 13,245 min): m/z (%) = 219 (M+1, 14), 218 (M^+, 100), 132 (17), 131 (87), 130 (23), 116 (9), 116 (20), 104 (17), 103 (16), 91 (6), 78 (10), 77 (13), 51 (5).

Compound 5f: ^{1}H-NMR (DMSO-d_6) δ (ppm) = 6,50 (s, 1H); 7,26 (t; J_1=8,92 Hz; 2H); 7,81 (dd; J_1=8,92 Hz; J_2=5,58 Hz; 2H). ^{13}C-NMR (DMSO-d_6) δ (ppm) = 110,47; 115,84 (J_2 $^{C\text{-}F}$=21,61 Hz; 2C); 127,75; 129,00; 132,51 (J_3 $^{C\text{-}F}$=8,18 Hz; 2C); 162,38 (J_1 $^{C\text{-}F}$=248,74 Hz); 165,78; 179,31. ^{19}F-NMR (DMSO-d_6) δ (ppm): -110,82. GC-MS (100-250 °C, 15 °C/min; R_t: 12,102 min): m/z = 223 (M+1, 12), 222 (M^+, 99), 136 (20), 135 (100), 134 (14), 108 (44), 116 (20), 107 (37), 86 (8), 59 (8).

Compound 5g: ^{1}H-NMR (acetone-d_6, 22ºC) δ (ppm): 6,71 (s, 1H); 7,18 (dd; J_1=4,91 Hz; J_2=3,72 Hz, 1H); 7,52 (d,t; J_1=3,72 Hz; J_2=0,66 Hz, 1H), 7,65 (d,t; J_1=4,91 Hz; J_2=0,66 Hz, 1H), 9,05 ($s_{(movil)}$, 1H); 10,04 ($s_{(movil)}$, 1H). ^{13}C-NMR (acetone-d_6) δ (ppm): 102,75; 128,86; 129,28; 130,05; 137,43; 155,05; 165,25. GC-MS (150-250 °C, 15 °C/min; R_t: 12,010 min): m/z (%) = 195 (M+1, 7), 194 (M^+, 70), 193 (3), 124 (12), 123 (100), 122 (40), 98 (4), 97 (13), 96 (75), 95 (21), 84 (4).

Compound 5h: ^{1}H-NMR (DMSO-d_6) δ (ppm) = 6,62 (s, 1H); 7,22 (dd; J_1=5,25 Hz; J_2=3,83 Hz, 1H); 7,81 (d,d; J_1=5,25 Hz; J_2=0,81 Hz, 1H), 7,86 (d,t; J_1=3,83 Hz; J_2=0,81 Hz, 1H), 10,97 ($s_{(movil)}$, 1H); 12,37 ($s_{(movil)}$, 1H). ^{13}C-NMR (DMSO-d_6) δ (ppm) = 104,30; 125,80; 129,16; 130,33; 130,63; 135,46; 165,47; 178,59. GC-MS (150-250 °C, 15 °C/min; R_t: 13,729 min): m/z (%)= 212 (M+2, 9), 212 (M+1, 11), 210 (M^+, 92), 125 (5), 131 (87), 124 (19), 123 (100), 122 (38), 97 (13), 96 (63), 95 (17), 86 (11).

Compound 5i: ^{1}H-NMR (DMSO-d_6) δ (ppm) = 6,48 (s, 1H); 7,28 (dd,d; J_1=7,44 Hz; J_2=4,80 Hz, J_3=1,44 Hz, 1H); 7,59 (d; J_1=7,66 Hz, 1H), 7,65 (t,d; J_1=7,66 Hz; J_2=1,44 Hz, 1H), 8,65 (d; J_1=4,80 Hz, 1H), 10,33 ($s_{(movil)}$, 1H); 11,29 ($s_{(movil)}$, 1H).^{13}C-NMR (DMSO-d_6) δ (ppm) = 104,91; 122,25; 125,40; 131,74; 137,06; 149,39; 153,66; 154,63; 165,10. GC-MS (100-250 °C, 15 °C/min; R_t: 7,318 min): m/z (%) = 190 (M+1, 6), 189 (M^+, 58), 146 (8), 118 (100), 91 (18), 78 (18), 64 (14), 51 (7).

Compound 5j: ^{1}H-NMR (DMSO-d_6) δ (ppm) = 6.61 (s, 1H); 7,38 (dd,d; J_1=7,72 Hz; J_2=4,82 Hz, J_3=1,07 Hz; 1H); 7,71 (d; J_1=7,72 Hz, 1H), 7,88 (t,d; J_1=7,72 Hz; J_2=1,80 Hz, 1H), 8,74 (d; J_1=4,82 Hz, 1H), 11,48 ($s_{(movil)}$, 1H); 12,51 ($s_{(movil)}$, 1H). ^{13}C-NMR (DMSO-d_6) δ (ppm): 107,30; 123,06; 126,50; 131,18; 137,36; 149,76; 153,12; 165,32; 178,42. GC-MS (100-250 °C, 15 °C/min; R_t: 12,771 min): m/z (%) = 206 (M+1, 11), 205 (M^+, 89), 172 (6), 162 (17), 146 (5), 119 (10), 118 (100), 104 (13), 91 (19), 81 (9), 78 (25), 64 (16), 63 (14), 51 (10).

Compound 5k: ^{1}H-NMR ($CDCl_3$) δ (ppm) = 3,09 (dd, J_1=14,01 Hz, J_2=8,37 Hz, 1H); 3,39 (dd, J_1=14,01 Hz, J_2=3,89 Hz, 1H); 4,54 (dd, J_1=8,37 Hz, J_2=3,89 Hz, 1H); 7,11 (d, J=1,25 Hz, 1H); 7,13 (d, J=1,76 Hz, 1H); 7,38 (m, 4H); 7,45 (m, 4H). GC-MS (150-250 °C, 10 °C/min; R_t: 17,37 min): m/z (%) = 282 (M+2, 3), 282 (M^+, 15), 136 (6), 135 (4), 92 (10), 91 (100).

Antioxidant assays

Samples preparation: All tests were performed with fixed concentrations of the synthesized compounds: 500, 250, and 100 µM in PBS with 0.4, 1 and 2 % of DMSO, respectively. The antioxidant standard Trolox was used as a positive control in all antioxidant tests at the same concentration as the samples. Equation 9 was used to calculate the free radical inhibition percentages of all tested samples. $Abs_{control}$ is the negative control (100%

free radical) absorbance value, and the $Abs_{reaction\ mixture}$ is the absorbance of the tested sample.

$$\%\ \text{Inhibition} = \frac{(Abs_{control} - Abs_{reaction\ mixture})}{Abs_{control}}\ 100\% \qquad \text{Eq. 9}$$

Antioxidant capacity evaluation by DPPH•: A solution of 0.40 µg/mL of DPPH• was diluted to adjust its absorbance to 0.80 ± 0.05 at 517 nm. The reaction mixture (300 µL), as well as its isolated components, were vigorously stirred with 2.70 mL of DPPH• solution. The samples were incubated at room temperature for 30 min, protected from light, for later spectrophotometric evaluation of absorbance (λ = 517 nm). Evaluation of antioxidant activity was performed in triplicate and the absorbance values were expressed as percentages of DPPH• production inhibition.

Antioxidant capacity evaluation by ABTS•+: The $ABTS^{\bullet+}$ was initially formed by the reaction between 950 mL of 7 mM ABTS solution and 17 mL of potassium persulfate ($K_2S_2O_8$) 2.45 mM, which was incubated at 8 °C for 16 h, protected from light. Then, the ABTS solution was diluted in purified water to obtain a solution with an absorbance of 0.80 ± 0.05, at 734 nm. Protected from light and at room temperature, 300 µL of different concentrations of testing samples were transferred to tubes containing 2.70 mL of $ABTS^{\bullet+}$ solution. Samples were read after 45 min by spectrophotometer (λ = 734 nm). The experiment was performed in triplicate and the results were expressed as a percentage of $ABTS^{\bullet+}$ production inhibition.

Reducing Power assay: The methodology described by Oyaizu et al.[39] served as a basis and minor modifications were made. The different concentration levels of the samples (300 µL) were mixed with phosphate buffer 0.2 M pH 6.6 (500 µL) and potassium ferricyanide $K_3[Fe(CN)_6]$ (500 µL). The mixture was incubated at 50 °C for 20 min. At room temperature, trichloroacetic acid (500 µL), purified water (950 µL), and $FeCl_3$ 0.1 %P/V (250 µL) were added and, finally, the absorbance was read at 700 nm. Equation 9 was used to calculate the increase in the reducing power of all tested samples. $Abs_{reaction\ mixture}$ is the absorbance of the tested sample and $Abs_{control}$ is the negative control (Prussian blue) absorbance value. If the testing compound has an antioxidant potential, then it can reduce Fe (III) from potassium ferricyanide, which leads to an increase of the absorption at 700 nm.

Statistical analysis of antioxidant assays: The data were expressed as mean ± standard deviation. Statistical analyses were performed by one-way ANOVA for multiple comparisons followed by the Student-Newman-Keuls test as a post hoc test. The results were considered statistically significant at $p \leq 0.05$. The Pearson correlation coefficient was used to assess the relationship between the results.

Microbiological studies

Strains and drugs: Intrinsic antimicrobial activity was tested against Gram-positive *(S. aureus* ATCC 25923) and Gram-negative (*Escherichia coli* ATCC 25922). Bacterial strains were maintained on Brain Heart Infusion Agar (BHIA, Himedia, India) slant at 4 ºC and, prior to assay, cells were grown overnight at 37 ºC in Brain Heart Infusion (BHI, Himedia, India).

Light-mediated antimicrobial activity: Assays for light-mediated antibacterial activity were performed in triplicate with the *S. aureus* ATCC 25923 and *E. coli* ATCC 25922 strains, according to Lopez et al. [40] Solutions of the imidazoline derivatives were prepared in DMSO (10000 µg/mL). Ten microliters of each solution were added in blank disks (100 µg/disk). The disks were placed on the surface of the medium previously inoculated with a bacterial suspension (approximately 1.5 x 108 CFU/mL). To monitor for light-activated antimicrobial activities, two replicate experiments were performed. One replicate plate was exposed to UV-A light (5 W/m2, 320-400 nm from four Sylvania F20T12-BLB lamps, maximum emission at 350 nm) for 2 h, while the other was kept in the dark. The plates were incubated at 37 ºC overnight and the inhibition zones were determined. As positive controls, a disk of ampicillin (10 µg/disk) was used as a standard antibiotic for bacteria. 8-methoxy-psoralen (8-MOP 5 µg/disk) dissolved in a hydro alcohol solution 40% (v/v) was utilized as a positive control requiring light for activation. Blank disks added with DMSO (10 µL) were used as a negative control. Species distribution, Log 1/S, LogP, and LogD were performed using the ACD/LabD and ACD/LogP (Advanced Chemistry Development Inc., Toronto, ON, Canada).

Statistical analysis: Each experiment was performed three times and the results were normalized by calculation of arithmetic average values. Statistical analysis was performed using a data bank from the statistical software SPSS (Statistical Package for Social Sciences), version 21. Assays were considered independent samples and were evaluated with a t-test of the mean, standard deviation, and standard errors of mean, using significance with $p \leq 0.05$.

Computational Methods

The molecular structure of each species was optimized at the DFT level using Gaussian 09.[41] The B3LYP (Becke three-parameter Lee-Yang-Parr) exchange-correlation functional was employed and the 6-311+G(d,p) basis set was used for the expansion of the Kohn-Sham orbitals of all the atoms. In order to check that the optimized geometry corresponds to a minimum in the potential energy surface, a frequency analysis at the same level of theory was computed. From the calculated total enthalpies, we have determined the following quantities:[42]

$$BDE = H(R^{\bullet}) + H(H^{\bullet}) - H(RH) \qquad \text{Eq. 10}$$

$$IP = H(RH^{\bullet+}) + H(e\text{-}) - H(RH) \qquad \text{Eq. 11}$$

Acknowledgments

The work at the Instituto de Investigaciones en Fisicoquímica de Córdoba (INFIQC) was supported by Consejo Nacional de Investigaciones Científicas y Técnicas (CONICET grant number: PIP 11220170100423CO), Fondo para la Investigación Científica y Tecnológica (FONCyT grant number: PICT-2017-1555), and Secretaría de Ciencia y Tecnología (SeCyT -UNC grant number: SeCyT-Nº411/18). This work used computational resources from CCAD-UNC (http://ccad.unc.edu.ar/), in particular the Mendieta Cluster, which is part of SNCAD-MinCyT. FAPEPI Grant 050/2019. MSF thanks the fellowship from CONICET.

Keywords: Antioxidants • Microwave chemistry • Imidazoline • *S. aureus* • Antibiotic resistance

[1] E. Szymańska, K. Kieć-Kononowicz, *IL FARMACO* **2002**, *57*, 355–362.
[2] L. Konnert, B. Reneaud, R. M. de Figueiredo, J.-M. Campagne, F. Lamaty, J. Martinez, E. Colacino, *J. Org. Chem.* **2014**, *79*, 10132–10142.
[3] J. C. Thenmozhiyal, P. T.-H. Wong, W.-K. Chui, *J. Med. Chem.* **2004**, *47*, 1527–1535.
[4] M. A. Khanfar, K. A. El Sayed, *Eur. J. Med. Chem.* **2010**, *45*, 5397–5405.

[5] C. V. Kavitha, M. Nambiar, C. S. Ananda Kumar, B. Choudhary, K. Muniyappa, K. S. Rangappa, S. C. Raghavan, *Biochem. Pharmacol.* **2009**, *77*, 348–363.
[6] S. Efendic, A. M. Efanov, P.-O. Berggren, S. V. Zaitsev, *Diabetes* **2002**, *51*, S448–S454.
[7] M. Singhal, A. Paul, H. P. Singh, *J. Saudi Chem. Soc.* **2011**, *18*, 121–127.
[8] M. Antolovich, P. D. Prenzler, E. Patsalides, S. McDonald, K. Robards, *Analyst* **2002**, *127*, 183–198.
[9] D. Huang, B. Ou, R. L. Prior, *J. Agric. Food Chem.* **2005**, *53*, 1841–1856.
[10] G. Firpo, M. L. Ramírez, M. S. Faillace, M. dos R. M. de Brito, A. P. S. C. L. e Silva, J. P. Costa, M. C. Rodríguez, G. A. Argüello, Z. Szakonyi, F. Fülöp, et al., *Antioxidants* **2019**, *8*, 197.
[11] M. R. M. de Brito, W. J. Peláez, M. S. Faillace, G. C. G. Militão, J. R. G. S. Almeida, G. A. Argüello, Z. Szakonyi, F. Fülöp, M. C. Salvadori, F. S. Teixeira, et al., *Toxicol. In Vitro* **2017**, *44*, 273–279.
[12] Ana P. Silva, José Carlos C. L. S. Filho, Joaquim S. da Costa Júnior, Walter J. Peláez, Martín S. Faillace, Alexandre de B. Falcão Ferraz, Jorge M. David, Rivelilson M. Freitas, *JPP* **2015**, *3*.
[13] A. Fabbretti, C. O. Gualerzi, L. Brandi, *FEBS Lett.* **2011**, *585*, 1673–1681.
[14] M. R. Hamblin, T. Hasan, *Photochem. Photobiol. Sci.* **2004**, *3*, 436–450.
[15] C.-F. Lee, C.-J. Lee, C.-T. Chen, C.-T. Huang, *J. Photochem. Photobiol., B* **2004**, *75*, 21–25.
[16] N. Kitamura, S. Kohtani, R. Nakagaki, *J. Photochem. Photobiol., C* **2005**, *6*, 168–185.
[17] H. H. Merritt, T. J. Putnam, *JAMA* **1938**, *111*, 1068–1073.
[18] R. P. Pohanish, in *Sittig's Handbook of Pesticides and Agricultural Chemicals (Second Edition)* (Ed.: R.P. Pohanish), William Andrew Publishing, Oxford, **2015**, pp. 483–506.
[19] S. Porwal, R. Kumar, P. R. Maulik, P. M. S. Chauhan, *Tetrahedron Lett.* **2006**, *47*, 5863–5866.
[20] T. Mendgen, C. Steuer, C. D. Klein, *J. Med. Chem.* **2012**, *55*, 743–753.
[21] B. Baum, A. L. Perun, *Polym. Eng. Sci.***1962**, *2*, 250–259.
[22] M. Eissen, J. O. Metzger, *Chem. - Eur. J.* **2002**, *8*, 3580–3585.
[23] A. J. Pepino, M. A. Burgos Paci, W. J. Peláez, G. A. Argüello, *Phys. Chem. Chem. Phys.* **2015**, *17*, 12927–12934.
[24] N. Nenadis, M. Z. Tsimidou, in *Measurement of Antioxidant Activity & Capacity*, John Wiley & Sons, Ltd, **2017**, pp. 141–164.
[25] B. Branchi, C. Galli, P. Gentili, *Org. Biomol. Chem.* **2005**, *3*, 2604–2614.
[26] G. I. Giles, K. M. Tasker, C. Jacob, *Free Radical Biology and Medicine* **2001**, *31*, 1279–1283.
[27] J. S. Wright, *J. Mol. Struct.: THEOCHEM* **2002**, *591*, 207–217.
[28] E. Klein, V. Lukeš, M. Ilčin, *Chem. Phys.***2007**, *336*, 51–57.
[29] J. S. Wright, E. R. Johnson, G. A. DiLabio, *J. Am. Chem. Soc.* **2001**, *123*, 1173–1183.
[30] W. Chen, P. Guo, J. Song, W. Cao, J. Bian, *Bioorg. Med. Chem. Lett.* **2006**, *16*, 3582–3585.
[31] W. Brand-Williams, M. E. Cuvelier, C. Berset, *LWT--Food Sci. Technol.* **1995**, *28*, 25–30.
[32] N. A. Kasim, M. Whitehouse, C. Ramachandran, M. Bermejo, H. Lennernäs, A. S. Hussain, H. E. Junginger, S. A. Stavchansky, K. K. Midha, V. P. Shah, et al., *Mol. Pharmaceutics* **2004**, *1*, 85–96.
[33] R. Apak, M. Özyürek, K. Güçlü, E. Çapanoğlu, *J. Agric. Food Chem.* **2016**, *64*, 997–1027.
[34] B. Y. Beker, T. Bakır, İ. Sönmezoğlu, F. İmer, R. Apak, *Chem. Phys. Lipids* **2011**, *164*, 732–739.
[35] P. A. Cerutti, *Science* **1985**, *227*, 375–381.
[36] M. V. Cooke, M. B. Oviedo, W. J. Peláez, G. A. Argüello, *Chemosphere* **2017**, *187*, 156–162.
[37] L. M. Costa, E. V. de Macedo, F. a. A. Oliveira, J. H. L. Ferreira, S. J. C. Gutierrez, W. J. Peláez, F. C. A. Lima, J. P. de S. Júnior, H. D. M. Coutinho, G. W. Kaatz, et al., *J. Appl. Microbiol.* **2016**, *121*, 1312–1322.
[38] N. F. Santos-Sánchez, R. Salas-Coronado, C. Villanueva-Cañongo, B. Hernández-Carlos, *Antioxidants* **2019**.
[39] M. Oyaizu, *Jpn. J. Nutr* **1986**, *44*.
[40] A. Lopez, J. B. Hudson, G. H. N. Towers, *J. Ethnopharmacol.* **2001**, *77*, 189–196.
[41] M. J. Frisch, G. W. Trucks, H. B. Schlegel, G. E. Scuseria, M. A. Robb, J. R. Cheeseman, G. Scalmani, V. Barone, B. Mennucci, G. A. Petersson, H. Nakatsuji, M. Caricato, X. Li, H. P. Hratchian, A. F. Izmaylov, J. Bloino, G. Zheng, J. L. Sonnenberg, M. Hada, M. Ehara, K. Toyota, R. Fukuda, J. Hasegawa, M. Ishida, T. Nakajima, Y. Honda, O. Kitao, H. Nakai, T. Vreven, J. A. Montgomery, Jr., J. E. Peralta, F. Ogliaro, M. Bearpark, J. J. Heyd, E. Brothers, K. N. Kudin, V. N. Staroverov, T. Keith, R. Kobayashi, J. Normand, K. Raghavachari, A. Rendell, J. C. Burant, S. S. Iyengar, J. Tomasi, M. Cossi, N. Rega, J. M. Millam, M. Klene, J. E. Knox, J. B. Cross, V. Bakken, C. Adamo, J. Jaramillo, R. Gomperts, R. E. Stratmann, O. Yazyev, A. J. Austin, R. Cammi, C. Pomelli, J. W. Ochterski, R. L. Martin, K. Morokuma, V. G. Zakrzewski, G. A. Voth, P. Salvador, J. J. Dannenberg, S. Dapprich, A. D. Daniels, O. Farkas, J. B. Foresman, J. V. Ortiz, J. Cioslowski, and D. J. Fox, Gaussian 09, Revision B.01, Gaussian, Inc., *Wallingford CT*, **2010**.
[42] M. Najafi, *J. Mex. Chem. Soc.* **2014**, *58*.

10.1002/cmdc.202000048

WILEY-VCH

FULL PAPER

A family of oxygenated and sulfurated imidazoline compounds was synthesized. Sulfur derivatives are better antioxidants than oxygenated counterparts. Moreover, these derivatives showed a light-enhanced activity against a *S. aureus* after irradiation with UV-A. The mechanisms of action are discussed in terms of the results, supported by DFT calculations.

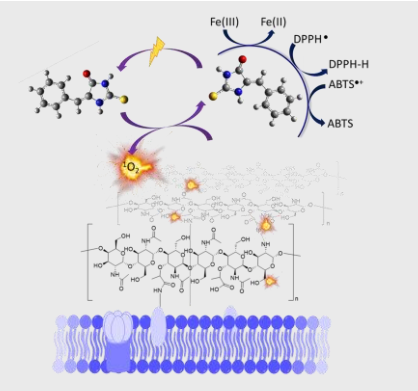

*Martín S. Faillace, Ana P. Silva, Antonio L. Alves Borges Leal, Luciana Muratori da Costa, Humberto M. Barreto, and Walter J. Peláez**

Page No. – Page No.

Sulfurated and oxygenated imidazoline derivatives: synthesis, antioxidant activity and light-mediated antibacterial activity